Global Health & Medicine. 2021; 3(2):73-81.
ORIGINAL ARTICLE
DOI: 10.35772/ghm.2020.01068

Epidemiological correlation between COVID-19 epidemic and prevalence of α-1 antitrypsin deficiency in the world

Hiroshi Yoshikura*

Emeritus Member, National Institute of Infectious Diseases, Tokyo, Japan

Abstract: Among 68 countries in the world, severity of the COVID-19 epidemic was correlated with the prevalence of α-1 antitrypsin (AAT) deficiency. For the severe variant, PI*Z, the correlation coefficient (CC) was 0.8584 for the number of patients and 0.8713 for the number of deaths. For the milder variant, PI*S, it was 0.5818 and 0.6326, respectively. In Japan, the number of patients and deaths correlated with the population size with a CC of 0.6667 and 0.7074 respectively, and was proportional to the population size to the power of 1.65 and 1.54. The prevalence of AAT deficiency also correlated with the epidemiological pattern of COVID-19. In countries with high prevalence of AAT deficiency, after the initial rise, the daily number of patients and that of deaths ran parallel at a high level for more than 6 months without sign of abatement. In countries with a low prevalence of AAT deficiency, after the first wave of the epidemic, the number of the deaths decreased continuously while the number of patients remained the same or even increased resulting in a decreasing case-fatality rate. When the cumulative number of deaths was plotted on the y-axis against the cumulative number of patients on the x-axis, plots fell on a straight line in countries with a high prevalence of AAT deficiency; while in countries with a low prevalence of AAT deficiency, a break appeared, after which the plots fell on flatter slope indicating decreasing case-fatality rate. The observation suggests emergence of an attenuated variant in countries with a low prevalence of AAT deficiency.

***Keywords*:** COVID-19, coronavirus, adaptation, quasi-species, case-fatality

Introduction

I was interested in why damage caused by COVID-19, epidemic of SARS-CoV-2, was so severe in countries in European and American continents despite of their advanced public health. I preliminarily examined the relation between COVID-19 and α-1 antitrypsin (AAT) deficiency, "a genetic disorder predominantly arising in those in European stock" according to Hutchinson (*1*). In the analysis, I used statistics on AAT deficiency published by de Serres *et al.* in 2012 (*2*). The number of the patients and that of the deaths (as of 19 May 2020) were correlated with the number of people with the more severe variant PI*Z of AAT deficiency with correlation coefficient (CC) 0.6049 and 0.6721, respectively. The correlation with the milder variant, PI*S, was 0.4207 and 0.4660 for patients and deaths respectively.

I recently found that Blanco *et al.* published new AAT deficiency statistics in 2017 (*3*). As the analysis strongly depends on the statistics of AAT deficiency, I reinvestigated the issue using the Blanco *et al.*'s statistics and the SARS-COV-2 data updated on 15 June 2020. I found the number of infections and that of the deaths due to SARS-CoV-2 infection were correlated with the prevalence of AAT deficiency with correlation coefficients of 0.8584 and 0.8713 for variant PI*Z, and 0.6326 and 0.5818 for PI*S, confirming my previous analysis.

The clinical manifestations of AAT deficiency varies widely from asymptomatic to fatal liver or lung diseases. As features suspicious of AAT deficiency, American Thoracic Society and the European Respiratory Society (ATS/ERS) counted early onset of emphysema (age of 45 years or less), emphysema in the absence of a recognized risk factor, emphysema with prominent basilar hyperlucency, and otherwise unexpected liver disease, *etc.* (*4*). For the clinical manifestation, tobacco smoking, exhaust gas, exposure to pathogens, *etc.* were known to be involved (*4*). Thus, AAT deficiency is "not a rare disease but a disease that is rarely diagnosed" (*5*).

AAT is a 52-kDa protein encoded by *SERPINA1* gene located in the 14th chromosome. The normal allele is coded as PI*M. The most frequent mutant alleles are PI*S and PI*Z, among which the deficiency was more severe for the latter. AAT is secreted from liver, and the protein encoded by the mutant alleles forms a polymer that is retained within hepatocytes resulting in the reduced serum level of AAT (*3*). According to the joint statement of ATS/ERS (*4*), the serum level (mg/dL) of AAT was 150-350 for PI*MM homozygotes (normal

individuals), 90-210 for PI*MZ heterozygotes, 100-200 for PI*SS homozygotes, 75-120 for PI*SZ heterozygotes, and 20-45 for PI*ZZ homozygotes. Estimated gene frequency per 1,000 population in Europe and the United States were respectively 1-9 and 2-4 for PI*S, and 2-24 and 1-2 for PI*Z (*4*). In Japan, AAT deficiency is listed among the "intractable diseases" (*6*), but the prevalence is < 1/1,000 population (*3*).

AAT counterbalances neutrophil elastase and other serine proteinases including trypsin. As we did not know which specific protease(s) are counterbalanced by anti-trypsin in the context of SARS-CoV-2 infection, protease(s) counterbalanced by anti-trypsin will be simply referred to as trypsin in this article.

The present study revealed an unexpected epidemiological correlation between the COVID-19 epidemic and AAT deficiency. The epidemiological data of COVID-19 used in this report were those from 21 January (report number 1, Rp1) to 26 June of 2020 (Rp158). As the COVID-19 pandemic progresses, new epidemiological features may emerge.

Materials and Methods

The COVID-19 epidemic data were derived from WHO Coronavirus disease (COVID-19) situation reports (*https://www.who.int/emergencies/diseases/novel-coronavirus-2019/situation-reports*) issued from 21 January 2020 to 18 June 2020, and the AAT deficiency prevalence data from tables published by Blanco *et al.* (*2*) (Table 1; Table S1-S2, *https://www.globalhealthmedicine.com/site/supplementaldata.html?ID=9*). The population size and population density data were derived from *https://www.worldometers.info/world-population/population-by-country* and *https://worldpopulationreview.com/country-rankings/countries-by-density* both downloaded on 20 July 2020. Age distribution of countries were derived from *https://data.worldbank.org/indicator/SP.POP.65UP.TO.ZS* downloaded on 20 July 2020.

Results

Correlation between AAT deficiency and COVID-19 morbidity and mortality

Table 1 lists the correlation coefficients (CC) between the number of people with AAT deficiency and the number of patients and deaths due to SARS-CoV-2 infection. The third column lists CCs for all analyzed countries combined. The fourth column CCs are for European and American countries, where 44 of 44 countries have a population with AAT deficiency. The fifth column CCs are for the remaining countries in other regions combined, of which 14 in 24 countries have a population with AAT deficiency variant PI*S, and 9 in 24 have a population with AAT deficiency variant PI*Z.

For all the countries combined, CC between the number of patients and the number of people with AAT deficiency PI*S, PI*Z or PI*SZ was 0.5818, 0.8584, and 0.7393, respectively, and CC between the number of deaths and the number of people with AAT deficiency was 0.6326, 0.8713, or 0.8585, respectively. When American and European countries were combined, excluding countries in the other regions, CC between the number of patients and the number of people with AAT deficiency PI*S, PI*Z or PI*SZ increased to 0.7594, 0.9170 and 0.7656, respectively; and CC between the number of deaths and the number of people with AAT deficiency PI*S, PI*Z or PI*SZ increased to 0.8244, 0.9503, and 0.8864. For the other regions however, CCs between the number of patients or deaths and the number of people with AAT deficiency became

Table 1. Correlation coeficients between COVI D-19 Morbidity or Mortality and Population with AAT Deficiency

AAT Deficiency	COVID-19	All (A + B)	Europe and America (A)	Other Regions (B)
PI*S	Patients	0.5818	0.7594	0.6670
	Deaths	0.6326	0.8244	0.4360
PI*Z	Patients	0.8584	0.9170	0.5697
	Deaths	0.8713	0.9503	0.4360
PI*SZ	Patients	0.7393	0.7656	0.0925
	Deaths	0.8585	0.8864	0.0253
Population size	Patients	0.3050	0.8941	0.6667
	Deaths	0.1701	0.8417	0.7074
> 65 years	Patients	0.3050	0.9038	0.4560
	Deaths	0.2701	0.8894	0.5403

European countries: Denmark, Estonia, Finland, Iceland, Latvia, Lithuania, Norway, Sweden, Belgium, France, Netherlands, Rep Ireland, United Kingdom, Austria, Germany, Poland, Switzerland, Italy, Portugal, Spain, North Macedonia, Russian Federation, Serbia.
American countries: Canada, USA, Mexico, Costa Rica, Cuba, Dominican Republic, El Salvador, Guatemala, Honduras, Nicaragua, Panama, Argentina, Bolivia, Brazil, Chile, Columbia, Ecuador, Paraguay, Peru, Uruguay, Venezuela.
African countries: Cameroon, Cape Verde, Morocco, Nigeria, Somalia, Tunisia, Democratic Republic Congo, Mozambique, Republic Congo, South Africa.
Asian countries: Kazakhstan, China, Indonesia, Japan, Malaysia, Mongolia, Papua New Guinea, Philippines, Singapore, Republic Korea, Thailand, Nepal, Pakistan, India.
Underlined countries are those with < 1/1,000 incidence both for PI*S and PI*Z.

almost insignificant.

Interestingly however, within each region, CC between the population size and the number of patients and number of deaths increased both for European and American countries and for countries in the other regions. European and American countries' CC was 0.8941 for the patients and 0.8417 for the deaths; and for countries in the other regions, CC was 0.6667 for the patients and 0.7074 for the deaths.

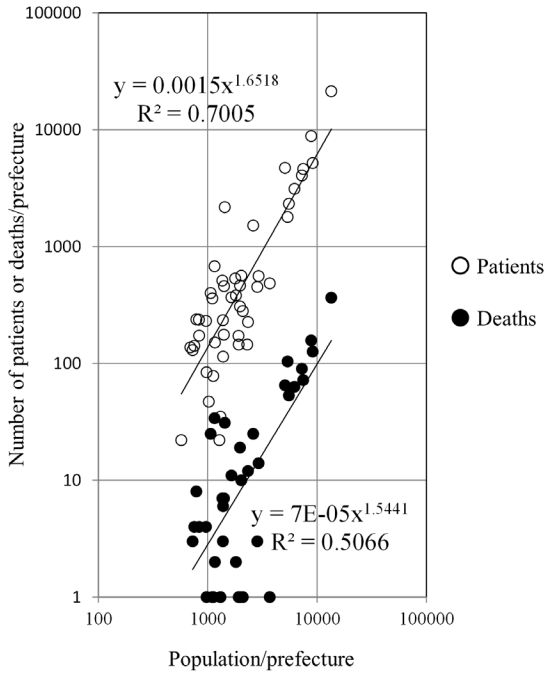

Figure 1. Relation between the number of the patients or the deaths due to SARS-COV-2 infection and the population size among 47 prefectures in Japan. The number of patients (○) or number of deaths (●) is plotted on the vertical axis and the population size of prefectures on the horizontal axis. Both axes are logarithmic scales. Prefectures with zero deaths were excluded from the plot for the deaths. CC was 0.8778 for the patients and 0.9062 for the deaths.

The above observation led me to suspect that infection of SARS-CoV-2 and accompanying deaths occurred almost at random within each group of the countries. Therefore I calculated the CC between the number of the SARS-CoV-2 patients or deaths (published in a daily newspaper Mainichi Shimbun, morning edition, on 4 September) and the population size among prefectures in Japan (Statistic bureau of Japan, *https://www.stat.go.jp/data/nihon/02.html*). CC between the number of patients and the population size was 0.8778, and CC between the number of deaths and the population size was 0.9062. I then plotted, on a logarithmic scale, the number of patients or deaths on the y-axis and the number of people on the x- axis for 47 prefectures in Japan. As shown in Figure 1, the relation between the number of patients (○) and the population size is represented by equation $y = 0.0015x^{1.652}$ with $R^2 = 0.7005$, and the relation between the number of deaths (●) and the population size by equation $y = 7E\text{-}05x^{1.544}$ with $R^2 = 0.5066$. The slope of the plots for COVID-19 is almost the same as for the measles epidemic (*7*), indicating that the COVID-19 epidemic is dependent on population size in the same way as the measles epidemic.

Figure 2 shows plots of the number of patients on the y-axis against the number of people with AAT deficiency variant PI*S (panel A), variant PI*Z (panel B) or the total population (panel C) on the x-axis for countries with AAT deficiency (> 1/1,000 population), which were mostly European and American countries.

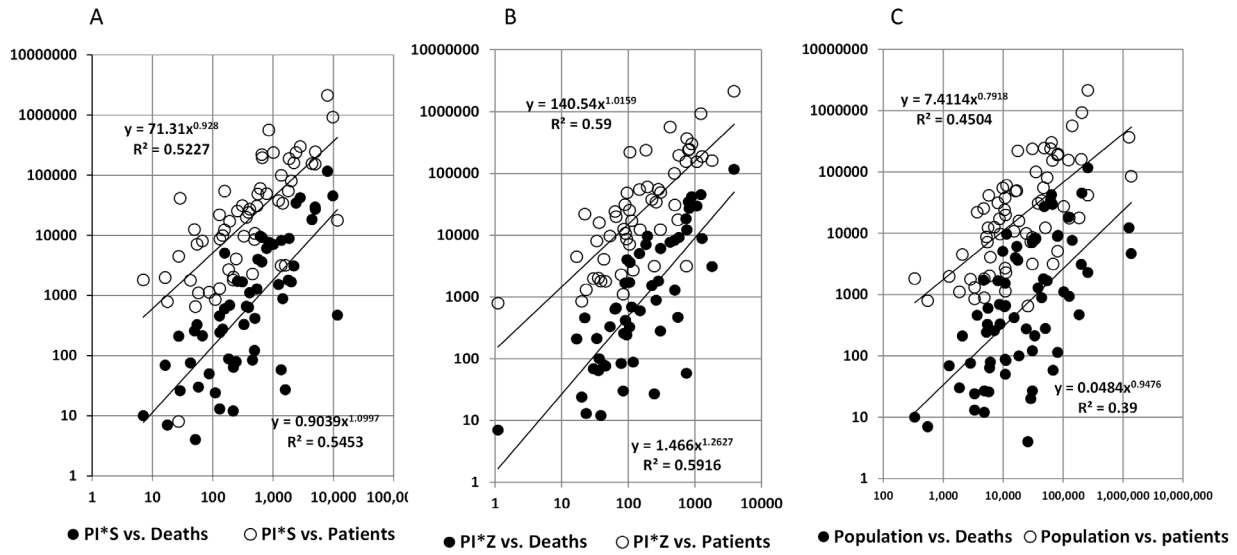

Figure 2. Relation between the number of the patients (○) or deaths (●) due to SARS-CoV-2 infection and the AAT deficient population among countries, panel A for variant PI*S, and panel B for variant PI*Z. Panel C shows the relation between the number of patients (○) or deaths (●) due to SARS-CoV-2 infection and population size (x1,000). The number of patients (○) or deaths (●) is plotted in the vertical axis and the population size of countries (x1,000) in the horizontal axis, both in the logarithmic scale. Countries with prevalence of AAT deficiency < 1/1,000 were excluded from this analysis.

The relation between the number of COVID-19 patients (y) and the AAT deficiency population (x) was expressed by equations $y = 140.54x^{1.02}$ with $R^2 = 0.59$ for PI*Z and $y = 71.31x^{0.93}$ with $R^2 = 0.52$ for PI*S; the relation between the number of COVID-19 deaths (y) and the AAT deficiency population (x) by equations $y = 1.466x^{1.26}$ with $R^2 = 0.59$ for PI*Z and $y = 0.9039x^{1.10}$ with $R^2 = 0.55$ for PI*S.

Epidemic curve of COVID-19

Figure 3A and B show plots of the daily number of new patients (open symbols) and new deaths (closed symbols) on a logarithmic scale from 21 January 2020 (Rp1 the first WHO situation report) to 26 June (Rp158). Also plotted, on a logarithmic scale, are the daily number of new deaths (D) divided by new infections (P), D/P, which is found in the area $y < 1$. Here, D/P is a parameter for monitoring the trends of new deaths relative to new infections. Curves obtained by the above plots will be called epidemic curves.

Through inspection of the epidemic curves, an epidemic model was constructed (see Table S3A for tabulation, *https://www.globalhealthmedicine.com/site/supplementaldata.html?ID=9*). In the model (Figure 5A), the plot for the number of patients and deaths are wave shaped; the peak of the deaths (●) is found on the right side of that of the patients (○). D/P decreases continuously until the number of patients reaches a peak; after that, if the number of patients (○) and deaths (●) decline, D/P increases towards the end of the epidemic (Δ); if the new infection stops decreasing in the middle (□) while the number of deaths continuously decreases (●), D/P declines again (◊).

With this model, countries fell into two groups. One is represented typically by China (Figure 3A). For China, there were three waves for patients, W1, W2 and W3, and one wave for deaths that dragged on from W1 (panel A in Figure 3A). For Rep Korea and Japan, there were two waves of patients, W1 and W2, and one wave of the deaths (panels B and C). D/P increased continuously until the transition between W1 and W2 (marked by a downward arrow) and then declined. Singapore and Malaysia (panel D) exhibited a similar pattern except the first wave of patients dragged on and the number of deaths declined continuously; as a consequence, D/P continuously decreased and faded away. The above countries all have a low prevalence of AAT deficiency. This plot pattern was shared by Morocco (prevalence of PI*S at 67/1,000 and that of PI*Z at 34/1,000) (*3*)) (panel E), United Arab Emirates (UAE) (prevalence of AAT deficiency unknown) (panel E), Cameroon (prevalence of PI*S at 146/1,000 and PI*Z at < 1/1,000) (*3*)) (panel F), DR Congo (prevalence of PI*S or PI*Z at < 1/1,000) (*3*)) (panel F), Kenya (prevalence of AAT deficiency unknown) (panel G) and Niger (prevalence of AAT deficiency unknown) (panels G).

Plots for Australia and New Zealand (panel H) were characterized by a pyramid-shaped wave of the number of patients and low number of deaths; D/P decreased first and then gradually increased and faded away. Australia and New Zealand are countries with a relatively high prevalence of AAT deficiency (PI*Z frequency 12.2/1,000 for Australia and 26/1,000 for New Zealand; PI*S frequency 42.2/1,000 for Australia and 33/1,000 for New Zealand) (*2*)).

The plot pattern was entirely different for countries with a high prevalence of AAT deficiency (Figure 3B). This pattern was shared by Sweden, Germany, Switzerland, Italy, Spain, United Kingdom (UK), Belarus, Russian Federation, France and Belgium in Europe (panels I-L); USA, Canada, Mexico, Peru, Chile, and Brazil in the Americas (panels M-N); and India, Bangladesh, Indonesia and Philippines (panels O-P). Among them, the countries in European and American continents have a high prevalence of PI*S, PI*Z or both (Table S1, *https://www.globalhealthmedicine.com/site/supplementaldata.html?ID=9*). Among the other countries, India has a high prevalence of PI*Z, Philippines has high prevalence of PI*S and Indonesia has prevalence < 1/1,000 both for PI*S and PI*Z (Table S2, *https://www.globalhealthmedicine.com/site/supplementaldata.html?ID=9*). Prevalence of AAT deficiency in Bangladesh is unknown.

Case vs. fatality plot

In Figure 4, the cumulative number of patients is plotted on the x-axis against the cumulative number of deaths on the y-axis, both on a logarithmic scale. Here, the plot starts from the date when the cumulative number of deaths exceeded 10 and started increasing continuously, because, in my preliminary study, I found that the number of deaths fluctuated aberrantly in the initial phase. Therefore, time range is indicated by the report number together with the country name, such as, China Rp40-87.

In principle, the case-fatality rate (CFR) does not change for a fixed pathogen and host pair. Therefore, the plot should expectedly fall on a straight line with slope of 1. This was not the case for many of the countries, however. For USA, the plot has a slope of 1.76, *i.e.*, the CFR increased continuously as the epidemic progressed (Figure 4D). For China, there was a break, after which the plot becomes flatter, *i.e.*, the CFR decreased progressively thereafter (Figure 4A). The virulence of viruses or the susceptibility of hosts does not change in such ways: what occurs is random mutation and selection. The above phenomena have to be explained in that context. "Two-population model" was developed for this purpose (*8*).

Simulation of the plot with a steep inclination angle (> 45°) is shown in Figure 5B and tabulation of the simulation in Table S3B (*https://www.*

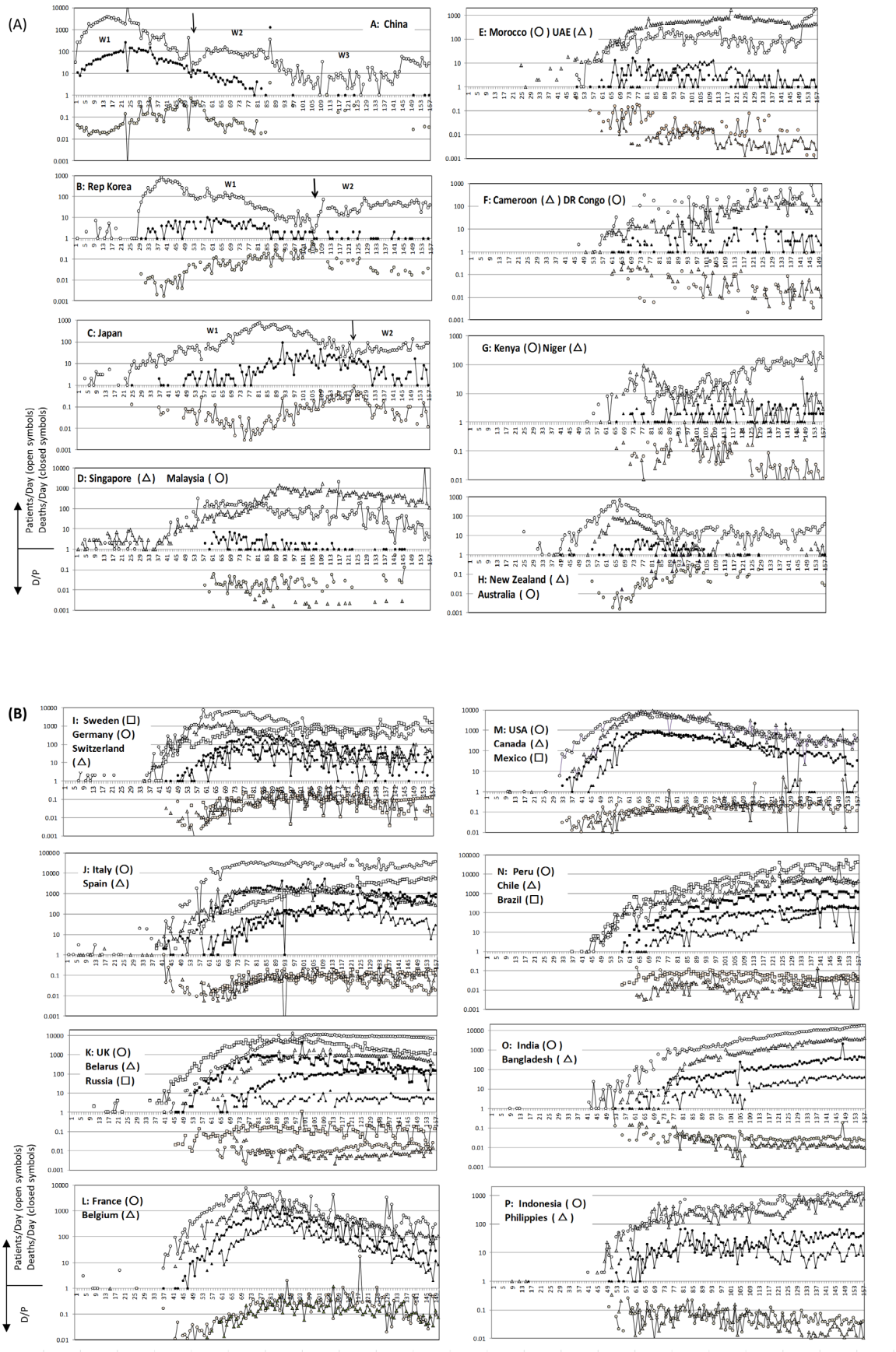

Figure 3. A and B, Epidemiological curves of COVID-19 for countries in various regions in the world. Daily incidence of new patients (open symbols) and new deaths (closed symbols) are plotted in the area y > 1; D/P (deaths/patient) is plotted in larger open symbols in the area y < 1.

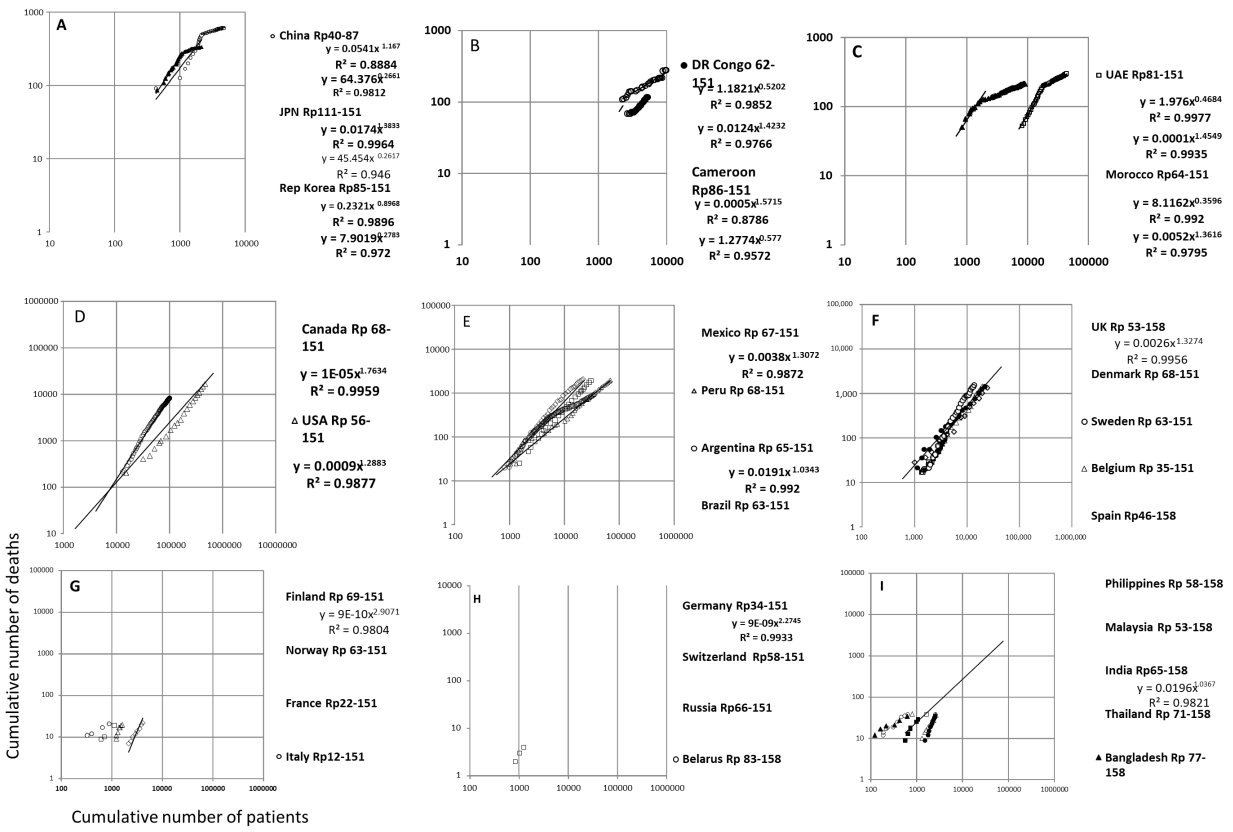

Figure 4. Case-fatality plots for various countries. The cumulative number of deaths is plotted on the vertical axis and cumulative number of patients on the horizontal axis, both on a logarithmic scale. The plot range is indicated by annotation, *e.g.*, Rp40-87 meaning that the plot range was from the WHO report number 40 to 87.

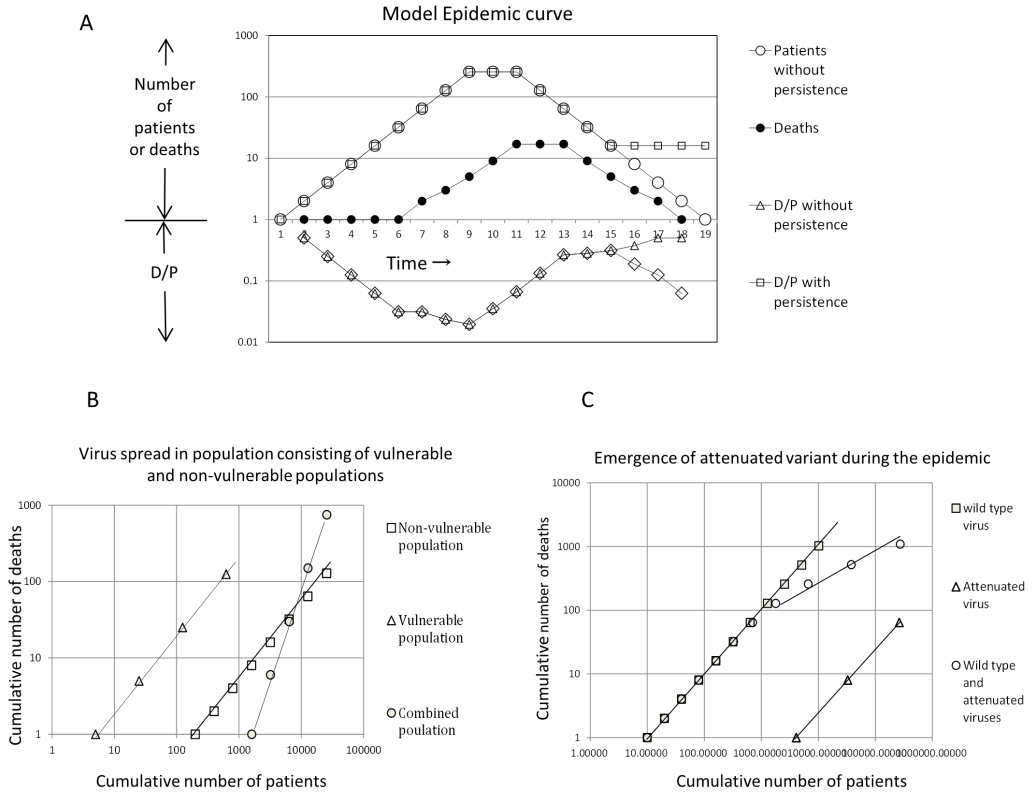

Figure 5. Model epidemic curve (A), case-fatality plot simulated for propagation of the virus in population consisting of vulnerable and non-vulnerable population (B), and simulated case-fatality plot for epidemic with emergent attenuated variant (C). Tabulation for the plot in panel A is found in Table S3A, that for panel B in Table S3B, and that for panel C in Table S3C. Explanations of symbols are found on the right side of the figures. See text for other details.

globalhealthmedicine.com/site/supplementaldata.html?ID=9). The model assumes that the population consists of a vulnerable minor subset (Δ), such as aged people in nursing homes, and a non-vulnerable major population (□); CFR is 1/5 for the former and 1/200 in the latter; and the speed of the spread is 2.5-fold more rapid for the former than for the latter. The 'Combined' column in Table S3B (*https://www.globalhealthmedicine.com/site/supplementaldata.html?ID=9*) is the number of patients or deaths in the vulnerable population and those of the non-vulnerable population added together. Plot of the added number of the patients on the x-axis against the added number of deaths on the y-axis both on a logarithmic scale (○) falls on a straight line with a slope of 1.4, which matches the steep slope plots for USA, Canada, Germany, Switzerland, *etc.* (Figure. 4D, 4F-4H); they are countries with a high population of elderly (population > 65 years was 16% for USA, 18% for Canada, and 22% for Germany). For Philippines, Malaysia, India, Thailand and Bangladesh (Figure 4I), Argentina and other countries in South America (Figure 4E) and Belarus (Figure 4H), the slope was near 1. These countries had a younger population (population > 65 years was 5% for Philippines and Bangladesh, 6% for India, 7% for Malaysia, 11% for Argentina, 12% for Thailand, and 15% for Belarus).

Simulation for the plot with a break is shown in Figure 5C and tabulation of the simulation in Table S3C (*https://www.globalhealthmedicine.com/site/supplementaldata.html?ID=9*). The simulation assumes that CFR of the wild type is 1/10 and that of the attenuated variant 1/4,096; in the middle of the epidemic (time 9 in Table S3C, *https://www.globalhealthmedicine.com/site/supplementaldata.html?ID=9*) of the wild type (□), the attenuated variant (Δ) emerges and spreads 4-fold more rapidly than the wild type. For the patients and deaths, the number for the wild type and the attenuated mutant are added together. The case-fatality plot for the two virus populations combined (○) initially has a slope of 1.0 but after the break its slope becomes 0.4. The model fits well with the plots for China, Rep Korea, and Japan, DR Congo, Cameroon, UAE and Morocco (Figure 4A-C).

Discussion

Among the reported countries, the number of patients and number of deaths due to SARS-CoV-2 infection correlate with the prevalence of variant PI*Z of AAT deficiency with a CC of 0.8584 and 0.8713, respectively. Correlation of the number of patients or deaths with the prevalence of PI*S is lower than that of PI*Z, which is reasonable because the serum level of α-1 antitrypsin is lower for PI*Z than for PI*S (AAT level relative to PI*MM was ~80% for PI*MS, 60% for PI*SS, 55% for PI*MZ, 40% for PI*SZ, and 15% for PI*ZZ (*2*)). Though AAT is an acute phase reactant, the pleomorphism of AAT was reflected in the normal time plasma level (*9*). Thus, the normal time plasma level should have strongly affected the outcome of SARS-CoV-2 infection. Recently Vianello and Braccioni reported geographical overlap between α-1 antitrypsin deficiency and SARS-CoV-2 infection in Italy (*10*).

The high correlation between the number of patients and deaths due to SARS-CoV-2 infection and the prevalence of AAT deficiency is equivalent to say that the propagation and pathogenicity of SARS-CoV-2 depends on exogenous trypsin, because, in people with a normal level of α1-antitrypsin, the level of active trypsin is kept in check by α1-antitrypsin, and viruses requiring trypsin remain under control, but in people with AAT deficiency, the trypsin level is not suppressed allowing for a high amount of trypsin to be available for the virus. Here, I used the term trypsin, but it could be other serine proteases, notably neutrophil elastase.

An important question is when and where the virus acquired property of trypsin dependency. In my own experience, trypsin-dependency emerged among mouse hepatitis virus released from normal looking carrier cells as an attenuated variant requiring trypsin (*11*) or coinfection with mouse leukemia virus (*12*) for plaque formation. Trypsin dependency will endow the virus with an increased chance to spread in populations with normal levels of AAT, because, although the replication of the virus in infected people may be slowed, the chance of the virus to spread will increase as infected people remain asymptomatic: it was reported that people asymptomatically infected by SARS-CoV-2 shed virus significantly longer than symptomatically infected patients (*13*). Therefore, I speculate that the trypsin dependency emerged as a process of adaptation to humans. Recently however, Wichit *et al.* reported that clinical isolate of porcine endemic diarrhea coronavirus required supplementation of exogenous trypsin (*14*). They argued that it was brought about by confinement of the natural infection of the virus in the protease-rich small intestine of pigs. Menachery *et al.* reported that a SARS-like coronavirus that bats harbor had the ability to infect humans without adaptation, but the virus needed exogenous protease treatment for isolation (*15*). Therefore, it is possible that SARS-CoV-2 was dependent on the exogenous trypsin before it was introduced into the human community.

In countries with a low prevalence of AAT deficiency, SARS-CoV-2 must have been experiencing attenuation because, in the case-fatality plots for China, Rep. Korea and Japan, there emerged a break followed by flatter plot resulting in decreasing fatality (Figure 4A). For China, the break was at Rp58 on 18 March 2020, and for Japan, it was at Rp131 on 29 May. Such a trend was also observed among DR Congo, Cameroon, UAE, and Morocco. They are not necessarily countries with a low prevalence of AAT deficiency, however.

The mutation involved in the attenuation could be

deletion in ORF8 observed among attenuated SARS virus in 2008 (*16*) or deletion in ORF3 for attenuated Middle East Respiratory Syndrome (*17*). The attenuated SARS mutant had reduced replication capacity, and could be recovered only by the reverse-genetics (*16*). It appeared that the mutant had an advantage in propagation on account of the reduced pathogenicity that permitted persistence in the host (*16*). It should be recalled that persistence is one of the important characteristics for successful propagation of viruses among hosts (*18*). Recently, attenuated variants of SARS-CoV-2 were obtained, which had a deletion in ORF7b and ORF8 (*19,20*) or in S1/S2 junction (*21*).

Though the above data suggests a strong correlation between the severity of the epidemic and the prevalence of AAT deficiency, there are some exceptions. For Indonesia, though AAT deficiency prevalence is < 1/1,000 (*3*), the number of patients and deaths were 41,431 and 2,276, respectively (Table S2, *https://www.globalhealthmedicine.com/site/supplementaldata.html?ID=9*). For Morocco, while the epidemiological curve resembled that of countries with a low prevalence of AAT deficiency, the prevalence of AAT deficiency was actually high (34/1,000 for PI*Z) and the number of patients and deaths were 8,020 and 213 respectively. Other exceptions were Australia and New Zealand: though the prevalence of AAT deficiency was high, the epidemiological curve resembled that of countries with low prevalence of AAT deficiency. In these countries, small population size and low population density may have played a role (for Australia, population size is 25,499,884 (55^{th} in the world) and population density 3/km sq. (226^{th} in the world); for New Zealand population size is 4,822,233 (126^{th} in the world) and population density is 18/km² (200^{th} in the world)). For spread of the virus in such a geographical environment, the mobility of infected people should have been critically important, and variants with lower virulence could have been selected for. Further exploration of the exceptional cases will lead to a better understanding of the relation between COVID-19 epidemics and AAT deficiency.

An important question not addressed above is the risk of COVID-19 deaths among populations with AAT deficiency relative to the risk among populations without. To answer this question, we have to know the frequency of AAT deficiency among COVID-19 patients and COVID-19 deaths. As there is currently no such information, it is not possible to answer this question. However, the following assessment could be possible. For example, if we suppose that the number of COVID-19 deaths per population in countries without AAT deficiency reflects the risk of deaths among the population without, it could be at most 0.074 ‰ (see column C5:D/Pop (‰) for Japan in Table S2, *https://www.globalhealthmedicine.com/site/supplementaldata.html?ID=9*). As "D/Pop (‰)" in Portugal with the highest prevalence of AATD was 1.405 ‰ (Table S1, *https://www.globalhealthmedicine.com/site/supplementaldata.html?ID=9*), the relative risk could be obtained by dividing 1.405‰ by 0.074‰, *i.e.*, 18.9-fold. As individuals with AAT deficiency occupied only 13.5% of the population in Portugal, the relative risk of the population with AAT deficiency could have been higher than that value. If all the fatality due to the SARS-CoV-2 infection was borne by the population with AAT deficiency in Portugal, relative risk could be calculated by dividing 18.9 by 0.135 to obtain 140-fold.

In conclusion, the COVID-19 epidemic was found to be under the influence of AAT deficiency globally, but within a region or in a country it depends on population size. It is important to note that the severity of the epidemic was influenced by other factors (*22-23*). The COVID-19 epidemic is still progressing as of early September 2020. The epidemiology of COVID-19 needs to be followed closely.

Acknowledgements

I acknowledge that the present study could not have been initiated without the data on prevalence of AAT deficiency compiled by F.J. Serres and I. Blanco. I thank Prof. Ignacio Blanco, Fundacion Registro Espanol del DAAT and Prof. Andrea Vianello, University of Padua for information and advice. I thank AIDS Research Center, National Institute of Infectious Disease for providing me with the space to conduct this research.

Funding: None.

Conflict of Interest: The author has no conflict of interest to disclose.

References

1. Hutchinson DC. Alpha 1-antitrypsin deficiency in Europe: geographical distribution of Pi types S and Z. Respir Med. 1998; 92:367-377.
2. de Serres FJ, Blanco I. Prevalence of α1-antitrypsin deficiency alleles PI*S and PI*Z worldwide and effective screening for 12each of the five phenotype classes PI*MS, PI*MZ, PI*SS, PI*SZ, and PI*ZZ: a comprehensive review. Ther Adv Respir Dis. 2012; 6:277-295.
3. Blanco I, Bueno P, Diego I, Pérez-Holanda S, Lara B, Casas-Maldonado F, Esquinas C, Miravitlles M. Alpha-1 antitrypsin Pi*SZ genotype: estimated prevalence and number of SZ subjects worldwide. Int J Chron Obstruct Pulmon Dis. 2017; 12:1683-1694.
4. American Thoracic Society; European Respiratory Society. American Thoracic Society/ European Respiratory Society statement: standards for diagnosis and management of individuals with alpha1-antitrypsin deficiency. Am J Respir Crit Care Med. 2003; 168:818-900.
5. de Serres FJ. Alpha-1 antitrypsin deficiency is not a rare disease but a disease that is rarely diagnosed. Environ Health Perspect. 2003; 111:1851-1854.

6. Ministry of Health Labour and Welfare. Intractable diseases designated on June 1 2015 – Notice number 111-306. *https://www.mhlw.go.jp/stf/seisakunitsuite/bunya/0000079293.html* (accessed August 10, 2020) (in Japanese).
7. Yoshikura H, Takeuchi. Population dependency of measles, syphilis, and amebiasis in Japan and community evolution. Jpn J Infec Dis. 2017; 70:263-269.
8. Yoshikura H. Two-population model accounting for the different patterns observed in the log-log plot of the cumulative numbers of those infected and killed in the early phase of the 2009 H1N1 pandemic in contrast to the one-population model accounting for the 1918-1919 pandemic in San Francisco. Jpn J Infec Dis. 2009; 62:482-483.
9. Luisetti M, Seersholm N. Alpha1- antitrypsin deficiency. 1: epidemiology of alpha1-antitrypsin deficiency. Thorax. 2004; 59:164-169.
10. Vianello A, Braccioni F. Geographical overlap between alpha-1 antitrypsin deficiency and COVID-19 infection in Italy: casual or causal? Arch Bronconeumol. 2020; 56:609-610.
11. Yoshikura H, Tejima S. Role of protease in mouse hepatitis virus-induced cell fusion. Studies with a cold-sensitive mutant isolated from a persistent infection. Virology. 1981: 113:503-511.
12. Yoshikura H, Taguchi F. Induction of lytic plaques by murine leukemia virus in murine sarcoma virus-transformed nonproducer mouse cells persistently infected with mouse hepatitis virus MHV-S. Intervirology. 1979; 11:69-73.
13. Long QX, Tang XJ, Shi QL. *et al*. Clinical and immunological assessment of asymptomatic SARS-CoV-2 infections. Nat Med. 2020; 26:1200-1204.
14. Wichit O, Li W, Willems L, Meuleman TJ, Wubbolts RW, van Kuppeveld FJ, Rottier PJ, Bosch BJ. Proteolytic activation of porcine epidemic diarrhea coronavirus spike fusion protein by trypsin in cell culture. J Virol. 2014; 88:7952-7961.
15. Menachery VD, Dinnon KH 3rd, Yount BL Jr, McAnarney ET, Gralinski LE, Hale A, Graham RL, Scobey T, Anthony SJ, Wang L, Graham B, Randell SH, Lipkin WI, Baric RS. Trypsin treatment unlocks barrier for zoonotic bat coronavirus infection. J Virol. 2020; 94:e01774-19.
16. Muth D, Corman VM, Roth H, *et al*. Attenuation of replication by a 29 nucleotide deletion in SARS coronavirus acquired during the early stages of human-to-human transmission. Scientific Rep. 2018; 8:15177.
17. Lamers MM, Stalin Raji V. Shafel M, Ali SS, Abdallh SM, Gazo M, Nofal S, Lu X, Erdman DD, Koopmans MP, Abdallat M, Haddadin A, Haagmans BL. Deletion variant of middle east respiratory syndrome coronavirus from humans, Jordan, 2015. Emerg Infect Dis. 2016; 22:716-719.
18. Vilarreal LP. The widespread evolutionary significance of viruses. Origin and Evolution of Viruses. 2008:477-516.
19. Su YCF, Anderson DE, Young BE, *et al.* Discovery and genome characterization of a 382-nucleotide deletion in ORF7b and ORF8 during the early evolution of SARS-CoV-2. mBio Jul. 2020; 11:e01610-20.
20. Young BE, Fong SW, Chan TM, *et al.* Effects of a major deletion in the SARS-CoV-2 genome on the severity of infection and the inflammatory response: an observational cohort study. Lancet. 2020; 396:603-611.
21. Lau SY, Wang P, Mok BW, Zhang AJ, Chu H, Lee AC, Deng S, Chen P, Chan KH, Song W, Chen Z, To KK, Chan JF, Yuen KY, Chen H. Attenuated SARS-CoV-2 variants with deletions at S1/S2 junction. Emerg Microbes Infect. 2020; 9:837-842.
22. Public Health England. Disparities in the risk and outcomes of COVID-19. *https://assets.publishing.service.gov.uk/government/uploads/system/uploads/attachment_data/file/908434/Disparities_in_the_risk_and_outcomes_of_COVID_August_2020_update.pdf* (accessed July 18, 2020).
23. Kuwahara K, Hori A, Ohmagari N, Mizoue T. Early cases of COVID-19 in Tokyo and occupational health. Global Health & Medicine. 2020; 2:118-122.

Received August 2, 2020; Revised September 7, 2020; Accepted September 15, 2020.

Released online in J-STAGE as advance publication October 12, 2020.

**Address correspondence to*:
Hiroshi Yoshikura, AIDS Research Center, National Institute of Infectious Diseases, 1-23-1, Toyama, Shinjuku-ku, Tokyo 162-8655, Japan.
E-mail: yoshikura@nih.go.jp